

Two-Photon Exchange and Elastic Electron-Proton Scattering

P. G. Blunden,^{1,2} W. Melnitchouk,² and J. A. Tjon^{2,3}

¹*Department of Physics and Astronomy, University of Manitoba, Winnipeg, Manitoba, Canada R3T 2N2*

²*Jefferson Lab, 12000 Jefferson Avenue, Newport News, Virginia 23606, USA*

³*Department of Physics, University of Maryland, College Park, Maryland 20742-4111, USA*

(Received 25 June 2003; published 3 October 2003)

Two-photon exchange contributions to elastic electron-proton scattering cross sections are evaluated in a simple hadronic model including the finite size of the proton. The corrections are found to be small in magnitude, but with a strong angular dependence at fixed Q^2 . This is significant for the Rosenbluth technique for determining the ratio of the electric and magnetic form factors of the proton at high Q^2 , and partly reconciles the apparent discrepancy with the results of the polarization transfer technique.

DOI: 10.1103/PhysRevLett.91.142304

PACS numbers: 25.30.Bf, 12.20.Ds, 13.40.Gp, 24.85.+p

The electromagnetic structure of the proton is reflected in the Sachs electric [$G_E(Q^2)$] and magnetic [$G_M(Q^2)$] form factors. The ratio $R = \mu_p G_E/G_M$, where μ_p is the proton magnetic moment, has been determined using two experimental techniques. The Rosenbluth, or longitudinal-transverse (LT), separation extracts R^2 from the angular dependence of the elastic electron-proton scattering cross section at fixed momentum transfer Q^2 . The results are consistent with $R \approx 1$ for $Q^2 < 6 \text{ GeV}^2$ [1,2]. However, recent polarization transfer experiments at Jefferson Lab [3] measure R from the ratio of the transverse to longitudinal polarizations of the recoiling proton, yielding the markedly different result $R \approx 1 - 0.135(Q^2 - 0.24)$ over the same range in Q^2 [1], which exhibits nonscaling behavior. In this Letter, we examine whether this discrepancy can be explained by a reanalysis of the radiative corrections, in particular, as they affect the LT separation analysis.

Consider the elastic ep scattering process $e(p_1) + p(p_2) \rightarrow e(p_3) + p(p_4)$. The Born amplitude for one photon exchange is given by

$$\mathcal{M}_0 = -i \frac{e^2}{q^2} \bar{u}(p_3) \gamma_\mu u(p_1) \bar{u}(p_4) \Gamma^\mu(q) u(p_2), \quad (1)$$

where the proton current operator is defined as

$$\Gamma^\mu(q) = F_1(q^2) \gamma^\mu + i \frac{F_2(q^2)}{2M} \sigma^{\mu\nu} q_\nu, \quad (2)$$

$q = p_4 - p_2 = p_1 - p_3$ is the four-momentum transferred to the proton ($Q^2 \equiv -q^2 > 0$), M is the proton mass, and F_1 and F_2 are linear combinations of the Sachs form factors G_E and G_M [see Eqs. (18) and (19)].

The resulting cross section depends on two kinematic variables, conventionally taken to be Q^2 (or $\tau \equiv Q^2/4M^2$) and either the scattering angle θ or the virtual photon polarization $\epsilon = [1 + 2(1 + \tau)\tan^2(\theta/2)]^{-1}$. It can be put in the form

$$d\sigma_0 = A[\tau G_M^2(Q^2) + \epsilon G_E^2(Q^2)], \quad (3)$$

where A depends on kinematic variables. This expression

is modified by radiative corrections, expressed in the form $d\sigma = d\sigma_0(1 + \delta)$. Usually δ is estimated by taking the one-loop virtual corrections of order α as well as the inelastic bremsstrahlung cross section for real photon emission.

The LT separation technique extracts the ratio $(G_E/G_M)^2$ from the ϵ dependence of the cross section at fixed Q^2 . With increasing Q^2 , the cross section is dominated by G_M , while the relative contribution of the G_E term is diminished. Hence, understanding the ϵ dependence in the radiative correction δ becomes increasingly important at high Q^2 . By contrast, the polarization transfer technique involves a ratio of cross sections, and is not expected to show the same sensitivity to the ϵ dependence of δ [4].

The amplitude \mathcal{M}_1 for the one-loop virtual corrections can be written as the sum of a ‘‘factorizable’’ term, proportional to the Born amplitude \mathcal{M}_0 , plus a remainder:

$$\mathcal{M}_1 = f(Q^2, \epsilon) \mathcal{M}_0 + \overline{\mathcal{M}}_1. \quad (4)$$

Hence, to first order in α ($\alpha = e^2/4\pi$),

$$\delta = 2f(Q^2, \epsilon) + 2 \frac{\text{Re}\{\mathcal{M}_0^\dagger \overline{\mathcal{M}}_1\}}{|\mathcal{M}_0|^2}. \quad (5)$$

The factorizable terms dominate, and include the electron vertex correction, vacuum polarization, and the infrared (IR) divergent parts of the proton vertex and two-photon exchange corrections. These terms are all essentially independent of hadronic structure. The hadronic model-dependent terms from the finite proton vertex and two-photon exchange corrections are expressed in $\overline{\mathcal{M}}_1$. These terms are small, and are generally ignored [5]. The finite proton vertex correction was analyzed recently by Maximon and Tjon [6], who found $\delta < 0.5\%$ for $Q^2 < 6 \text{ GeV}^2$. It does not show a significant ϵ dependence, and so we drop it here.

The factorizable terms can be classified further. Each of the functions $f(Q^2, \epsilon)$ for the electron vertex, vacuum

polarization, and proton vertex terms depend only on Q^2 , and therefore have no relevance for the LT separation aside from an overall normalization factor. Hence, of the factorizable terms, only the IR divergent two-photon exchange contributes to the ϵ dependence of the virtual photon corrections.

For the inelastic bremsstrahlung cross section, the amplitude for real photon emission can also be written in the form of Eq. (4). In the soft photon approximation, the amplitude is completely factorizable. A significant ϵ dependence arises due to the frame dependence of the angular distribution of the emitted photon. These corrections, together with external bremsstrahlung, contain the main ϵ dependence of the radiative corrections, and are accounted for in the experimental analyses [2].

In principle, the two-photon exchange contribution to \mathcal{M}_1 , denoted $\mathcal{M}^{\gamma\gamma}$, includes all possible hadronic intermediate states (Fig. 1). Here we consider only the elastic contribution to the full response function, and assume that the proton propagates as a Dirac particle. We also assume that the off-shell current operator is given by (2), and use phenomenological form factors at the γp vertices. Clearly this creates a tautology, as the radiative corrections are also used to determine the experimental form factors. However, because δ is a ratio, the model dependence cancels somewhat, provided we use the same phenomenological form factors for both \mathcal{M}_0 and $\mathcal{M}^{\gamma\gamma}$ in Eq. (5).

The sum of the two-photon exchange box and crossed box diagrams has the form

$$\mathcal{M}^{\gamma\gamma} = e^4 \int \frac{d^4k}{(2\pi)^4} \left[\frac{N_a(k)}{D_a(k)} + \frac{N_b(k)}{D_b(k)} \right], \quad (6)$$

where the numerators are the matrix elements

$$\begin{aligned} N_a(k) &= \bar{u}(p_3) \gamma_\mu (\not{p}_1 - \not{k}) \gamma_\nu u(p_1) \\ &\quad \times \bar{u}(p_4) \Gamma^\mu (q - k) (\not{p}_2 + \not{k} + M) \Gamma^\nu (k) u(p_2), \end{aligned} \quad (7)$$

$$\begin{aligned} N_b(k) &= \bar{u}(p_3) \gamma_\nu (\not{p}_3 + \not{k}) \gamma_\mu u(p_1) \\ &\quad \times \bar{u}(p_4) \Gamma^\mu (q - k) (\not{p}_2 + \not{k} + M) \Gamma^\nu (k) u(p_2), \end{aligned} \quad (8)$$

and the denominators are the products of the scalar propagators,

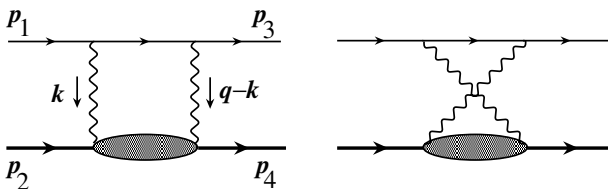


FIG. 1. Two-photon exchange box and crossed box diagrams.

$$\begin{aligned} D_a(k) &= [k^2 - \lambda^2][(k - q)^2 - \lambda^2] \\ &\quad \times [(p_1 - k)^2 - m^2][(p_2 + k)^2 - M^2], \end{aligned} \quad (9)$$

$$D_b(k) = D_a(k)|_{p_1 \rightarrow p_3 + k}. \quad (10)$$

An infinitesimal photon mass λ has been introduced in the photon propagator to regulate the IR divergences, and the electron mass m is ignored in the numerator.

The implementation of Eq. (6) is the main result of this Letter. However, we also want to compare with previous work, so a partial analysis of the leading terms in (6) is warranted.

To proceed, we can separate out the IR divergent parts from the finite ones. There are two poles in the integrand of (6) where the photons are soft: one at $k = 0$, and another at $k = q$. For the box diagram, the matrix element can be written as the sum of a contribution at the pole $k = 0$ plus a remainder, $N_a(k) = N_a(0) + \bar{N}_a(k)$. Explicitly, we have

$$N_a(0) = 4p_1 \cdot p_2 q^2 i \mathcal{M}_0 / e^2. \quad (11)$$

The matrix element at the pole $k = q$ is the same, so $N_a(q) = N_a(0)$ (this also follows from symmetry arguments). This suggests that the dominant contribution to the box amplitude can be approximated as

$$\mathcal{M}_a^{\gamma\gamma} \approx e^4 N_a(0) \int \frac{d^4k}{(2\pi)^4} \frac{1}{D_a(k)} \equiv \mathcal{M}_a^{\text{IR}}. \quad (12)$$

There are two assumptions implicit in this approximation. The first is that the integral involving $\bar{N}_a(k)$ is small, and contains no ultraviolet (UV) divergences from the F_2 part of the current operator (2). Without hadronic form factors, Eq. (2) does in fact lead to UV divergences. We demonstrate below how to get around this difficulty by rewriting F_1 and F_2 in terms of the Sachs form factors G_E and G_M . The second assumption is that the hadronic form factors have no significant effect on the loop integral, and can be factored out. In essence, this assumes that the hadronic current operators occurring in Eq. (6) can be replaced by $\Gamma^\mu(0) = \gamma^\mu$ for the vertex involving the soft photon, and by $\Gamma^\mu(q)$ for the other vertex.

With these caveats in mind, the IR divergent box amplitude from the pole terms can now be written as [6]

$$\begin{aligned} \mathcal{M}_a^{\text{IR}} &= \frac{\alpha}{\pi} p_1 \cdot p_2 q^2 \mathcal{M}_0 \frac{i}{\pi^2} \int d^4k \frac{1}{D_a(k)} \\ &= -\frac{\alpha}{\pi} \ln\left(\frac{2p_1 \cdot p_2}{mM}\right) \ln\left(\frac{Q^2}{\lambda^2}\right) \mathcal{M}_0. \end{aligned} \quad (13)$$

The four-point function arising from the loop integral has been evaluated analytically in the limit $\lambda^2 \ll Q^2$ following 't Hooft and Veltman [7].

A similar analysis of the crossed box amplitude shows that

$$N_b(0) = 4p_3 \cdot p_2 q^2 i \mathcal{M}_0 / e^2, \quad (14)$$

and, hence,

$$\mathcal{M}_b^{\text{IR}} = \frac{\alpha}{\pi} \ln\left(\frac{2p_3 \cdot p_2}{mM}\right) \ln\left(\frac{Q^2}{\lambda^2}\right) \mathcal{M}_0. \quad (15)$$

In the lab frame ($p_1 \cdot p_2 = E_1 M$ and $p_3 \cdot p_2 = E_3 M$), the total IR divergent two-photon exchange contribution to the cross section is readily seen to be

$$\delta_{\text{IR}} = -2 \frac{\alpha}{\pi} \ln\left(\frac{E_1}{E_3}\right) \ln\left(\frac{Q^2}{\lambda^2}\right), \quad (16)$$

a result given by Maximon and Tjon [6]. The logarithmic terms in m cancel in the sum, while the logarithmic IR singularity in λ is exactly canceled by a corresponding term in the bremsstrahlung cross section involving the interference between real photon emission from the electron and from the proton.

By contrast, in the standard treatment of Mo and Tsai (MT) [5], the loop integral in (13) is approximated by setting the photon propagator not at a pole equal to $1/q^2$. This results in a three-point function $K(-p_1, p_2)$ which, unfortunately, has no simple analytic form in the limit $\lambda^2 \ll Q^2$. After a further approximation $K(-p_1, p_2) \approx K(p_1, p_2)$, the total IR divergent result is given as [5]

$$\delta_{\text{IR}}(\text{MT}) = -2 \frac{\alpha}{\pi} [K(p_1, p_2) - K(p_3, p_2)], \quad (17)$$

where $K(p_i, p_j) = p_i \cdot p_j \int_0^1 dy \ln(p_y^2/\lambda^2)/p_y^2$ and $p_y = p_i y + p_j(1-y)$.

Because $\delta_{\text{IR}}(\text{MT})$ is the result generally used in existing experimental analyses [1,2], it is useful to compare the ϵ dependence with that of δ_{IR} . The difference $\delta_{\text{IR}} - \delta_{\text{IR}}(\text{MT})$ is independent of λ , and is shown in Fig. 2 as a function of ϵ for $Q^2 = 3 \text{ GeV}^2$ and $Q^2 = 6 \text{ GeV}^2$. The different treatments of the IR divergent terms already have significance for the LT separation, resulting in roughly a 1% change in the cross section over the range of ϵ . This effect alone gives a reduction of the order of 3% and 7% in the ratio R for $Q^2 = 3 \text{ GeV}^2$ and $Q^2 = 6 \text{ GeV}^2$, respectively.

We return now to the implementation of the full expression of Eq. (6). The full expression includes both finite

and IR divergent terms (there is no need to treat them separately), and form factors at the γp vertices. To avoid sensitivity to the UV divergences in the loop integrals arising from the F_2 part of the current operator (2), we rewrite F_1 and F_2 in terms of the Sachs form factors,

$$F_1(q^2) = \frac{G_E(q^2) + \tau G_M(q^2)}{1 + \tau}, \quad (18)$$

$$F_2(q^2) = \frac{G_M(q^2) - G_E(q^2)}{1 + \tau}. \quad (19)$$

G_E and G_M are taken to have the common form factor dependence $G_E(q^2) = G_M(q^2)/\mu_p \equiv G(q^2)$, with $G(q^2)$ a simple monopole $G(q^2) = -\Lambda^2/(q^2 - \Lambda^2)$. We leave a fuller exploration of the hadronic model dependence to a future paper. Effectively, the F_2 part of the current then behaves similar to a dipole, and the loop integrals are UV finite for any choice of cutoff mass Λ . We have taken $\Lambda = 0.84 \text{ GeV}$, consistent with the size of the nucleon, for which the results show a plateau of stability. The sensitivity to Λ is mild because the form factor dependence enters as a ratio in δ .

The loop integrals in Eq. (6) can be evaluated analytically in terms of four-point Passarino-Veltman functions [8], and trace techniques used to implement the sum over Dirac spinors implicit in Eq. (5). This is a formidable task that is facilitated by the use of established algebraic manipulation routines. We used two independent packages (FEYNALCALC [9] and FORMCALC [10]), which gave identical numerical results. The Passarino-Veltman functions were evaluated numerically using the FF program [11].

The model-independent IR divergent result of Eq. (16) is an appropriate benchmark with which to compare the full result δ_{full} . Because the IR behavior is the same, the difference $\delta_{\text{full}} - \delta_{\text{IR}}$ is finite (i.e., independent of λ). The results are shown in Fig. 3. A significant ϵ dependence is observed, which increases slightly with Q^2 . The additional correction is largest at backward

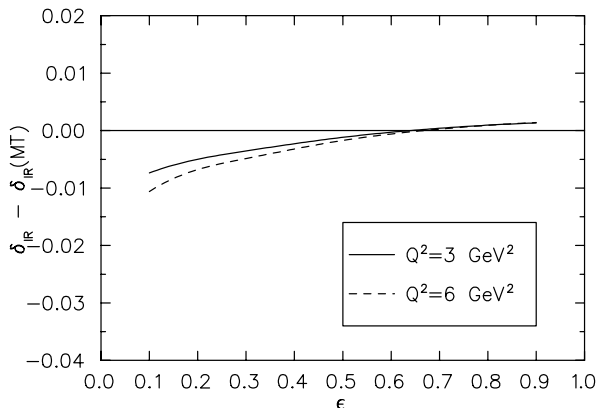


FIG. 2. Difference between the model-independent IR divergent contributions of Eq. (16) and of the commonly used expression (17).

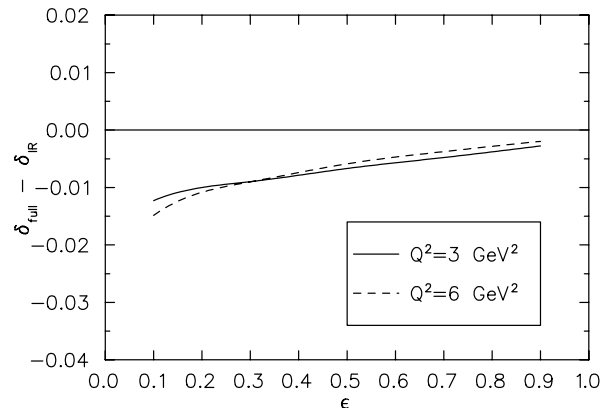


FIG. 3. Difference between the full two-photon exchange correction and the model-independent IR divergent result of Eq. (16).

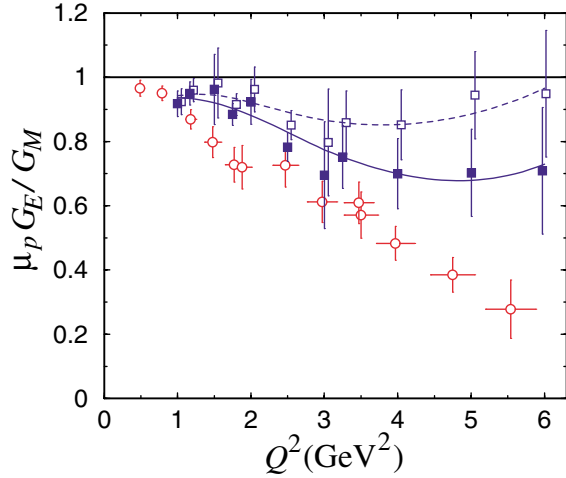


FIG. 4 (color online). The ratio of form factors measured using LT separation (hollow squares), together with the global fit (dashed line). The unshifted LT data represent a binned average of all LT separated data points with normalization factors determined by the global fit in Ref. [1]. Filled squares show the shift in the LT results due to the two-photon exchange corrections (offset for clarity), and the solid line shows the effect on the global fit. Error bars have been left unchanged. The polarization transfer data [3] are shown as hollow circles.

angles ($\epsilon \rightarrow 0$), and essentially vanishes at forward angles ($\epsilon \rightarrow 1$).

To consider the effect on the ratio R determined in the LT separation, we make a simplified analysis that assumes the modified cross section is still approximately linear in ϵ . The results shown in Figs. 2 and 3 are combined, giving $\Delta = \delta_{\text{full}} - \delta_{\text{IR}}(\text{MT})$. For each value of Q^2 in the range 1–6 GeV^2 , we fit the correction $(1 + \Delta)$ to a linear function of ϵ of the form $a(1 + b\epsilon)$. The parameter b so determined behaves roughly like $b \approx 0.014 \ln(Q^2/0.65)$, with Q^2 in GeV^2 . For the LT separation, the corrected Eq. (3) becomes

$$d\sigma = (aA)\tau G_M^2(Q^2)[1 + (B\tilde{R}^2 + b)\epsilon], \quad (20)$$

where $B = 1/(\mu_p^2\tau)$, and \tilde{R} is the corrected ratio R . Since $a \approx 1$, we have essentially $\tilde{R}^2 = R^2 - b/B$.

The shift in R is shown in Fig. 4, together with the polarization transfer data. The effect of the additional terms is significant. Although some dependence on nucleon structure is expected, these calculations show that the two-photon corrections have the proper sign and magnitude to resolve a large part of the discrepancy between the two experimental techniques. Clearly, there is room for additional contributions from inelastic nucleon excitation (e.g., the Δ^+). These have been examined previously in Ref. [12] in various approximations. Greenhut [12] used a fit to proton Compton scattering to calculate the resonant contribution to two-photon exchange, and found some degree of cancellation with the nonresonant terms at high energies. Further study of the

inelastic region is required, including also the imaginary part of the response function [13].

Direct experimental evidence for the contribution of the real part of two-photon exchange can be obtained by comparing e^+p and e^-p cross sections. (\mathcal{M}_0 changes sign under $e^- \rightarrow e^+$, whereas $\mathcal{M}^{\gamma\gamma}$ does not.) Hence, we expect to see an enhancement of the ratio $\sigma(e^+p)/\sigma(e^-p)$ due to two-photon exchange (after the appropriate IR divergences are canceled due to bremsstrahlung). There are experimental constraints from data taken at SLAC [14] for $E_1 = 4 \text{ GeV}$ and $E_1 = 10 \text{ GeV}$, which are consistent with our results. However, the SLAC data are from forward scattering angles, with $\epsilon > 0.72$, where we find the two-photon exchange contribution is $\lesssim 1\%$. A more definitive test of the two-photon exchange mechanism could be obtained at backward angles, where an enhancement of the order of a few percent is predicted.

We thank A. Afanasev, J. Arrington, S. Brodsky, K. de Jager, and R. Segel for helpful discussions. P.G.B. also thanks the theory group and Hall C at Jefferson Lab for support during a sabbatical leave, where this project was undertaken. This work was supported in part by NSERC (Canada), DOE Grant No. DE-FG02-93ER-40762, and DOE Contract No. DE-AC05-84ER-40150 under which SURA operates the Thomas Jefferson National Accelerator Facility.

-
- [1] J. Arrington, Phys. Rev. C (to be published).
 - [2] R. C. Walker *et al.*, Phys. Rev. D **49**, 5671 (1994); L. Andivahis *et al.*, Phys. Rev. D **50**, 5491 (1994).
 - [3] M. K. Jones *et al.*, Phys. Rev. Lett. **84**, 1398 (2000); O. Gayou *et al.*, Phys. Rev. Lett. **88**, 092301 (2002).
 - [4] L. C. Maximon and W. C. Parke, Phys. Rev. C **61**, 045502 (2000); A. Afanasev *et al.*, Phys. Lett. B **514**, 269 (2001).
 - [5] L. W. Mo and Y. S. Tsai, Rev. Mod. Phys. **41**, 205 (1969); Y. S. Tsai, Phys. Rev. **122**, 1898 (1961).
 - [6] L. C. Maximon and J. A. Tjon, Phys. Rev. C **62**, 054320 (2000).
 - [7] G. 't Hooft and M. J. Veltman, Nucl. Phys. B **153**, 365 (1979).
 - [8] G. Passarino and M. J. Veltman, Nucl. Phys. B **160**, 151 (1979).
 - [9] R. Mertig, M. Bohm, and A. Denner, Comput. Phys. Commun. **64**, 345 (1991); <http://www.feyncalc.org>.
 - [10] T. Hahn and M. Perez-Victoria, Comput. Phys. Commun. **118**, 153 (1999); <http://www.feynarts.de>.
 - [11] G. J. van Oldenborgh and J. A. M. Vermaseren, Z. Phys. C **46**, 425 (1990); <http://www.nikhef.nl/~t68/ff>.
 - [12] S. D. Drell and M. Ruderman, Phys. Rev. **106**, 561 (1957); S. D. Drell and S. Fubini, Phys. Rev. **113**, 741 (1959); J. A. Campbell, Phys. Rev. **180**, 1541 (1969); G. K. Greenhut, Phys. Rev. **184**, 1860 (1969).
 - [13] A. Afanasev, I. Akushevich, and N. P. Merenkov, arXiv:hep-ph/0208260.
 - [14] J. Mar *et al.*, Phys. Rev. Lett. **21**, 482 (1968).